Electrical, magnetic, and optical properties of the tetrathiafulvalene (TTF) pseudohalides, $(TTF)_{12}(SCN)_7$ and $(TTF)_{12}(SeCN)_7$†

R. B. Somoano, A. Gupta, and V. Hadek
Jet Propulsion Laboratory, Pasadena, California 91103

M. Novotny
Physics Department, Stanford University, Stanford, California 94305

M. Jones, T. Datta, R. Deck, and A. M. Hermann
Physics Department, Tulane University, New Orleans, Louisiana 70118

(Received 22 March 1976)

The electrical, magnetic, and optical properties of charge-transfer salts containing tetrathiafulvalene (TTF) and the pseudohalides, thiocyanate (SCN) and selenocyanate (SeCN), have been investigated. These salts are quasi-one-dimensional compounds containing cation radicals only, in contrast to a cation-radical–anion-radical system, such as tetrathiafulvalene tetracyanoquinodimethane (TTF) (TCNQ). Measurements of electrical conductivity, thermoelectric power, and optical reflectivity of single crystals of the nonstoichiometric salts $(TTF)_{12}(SCN)_7$ and $(TTF)_{12}(SeCN)_7$ show metal-like characteristics above 200°K (high-temperature region). The conductivities at room temperature are $\sim 750\ \Omega^{-1}\text{cm}^{-1}$, comparable to those found in (TTF) (TCNQ), and increase with decreasing temperature down to ~ 200°K. The thermoelectric power at room temperature is small and positive ($\sim 9\ \mu\text{V/°K}$), and decreases linearly with decreasing temperature in this region (as expected for metal-like hole conduction along the TTF chains). The ESR intensity, however, decreases with decreasing temperature above 200°K. At 170°K a metal-nonmetal transition occurs, and the transport and magnetic properties below this temperature are characteristic of a semiconducting state.

INTRODUCTION

The exciting discovery of high conductivity in organic charge-transfer salts containing TCNQ (tetracyanoquinodimethane) has produced a stimulus for extensive investigation of the electronic properties of quasi-one-dimensional materials.[1] The high conductivity is due in large measure to the orbital overlap of carbon $2p\pi$ orbitals of TCNQ anion radicals stacked in columnar fashion. Considerably enhanced conductivities have recently been observed in the quasi-one-dimensional organic charge-transfer salt containing TCNQ anion radicals and TTF (tetrathiafulvalene) cation-radical chains where in the latter the contribution of the larger sulfur $3p\pi$ orbitals to band formation should be significant.[2] The presence of both types of carriers in (TTF) (TCNQ)-type structures complicates the interpretation of the experimental data. Some recent investigations have been made on highly-conducting TTF cation-radical salts containing halogen anions instead of TCNQ anion radicals.[3-6] The conductivity of these materials is along the TTF chains only, which simplifies the interpretation of the data and provides an opportunity to study the contribution of heteroatoms to the electronic transport properties. However, the (TTF) (halide) salts usually yield crystals which are twinned and highly defective, and consequently the intrinsic properties are partially obscured.

In this paper, we present the results of electrical, magnetic, and optical measurements made on cation-radical structures containing TTF and the pseudohalides, SCN^- and $SeCN^-$. These salts yield crystals superior to those obtained with the halides and have conductivities comparable to that of (TTF)(TCNQ). Because of the chemical nature of pseudohalides, one would expect negligible back charge transfer to occur and the degree of band filling may therefore be computed. This latter feature along with the single-carrier nature and the structural similarity to the TTF halides have provided the impetus for this study.

EXPERIMENTAL

TTF was synthesized according to techniques published in the literature[7] and purified by multiple recrystallization and gradient sublimation. Conversion to the fluoroborate salt $(TTF)_3(BF_4)_2$, which is required due to the unavailability of SCN^0 and $SeCN^0$, was accomplished by the method of Wudl[6] and was followed by recrystallization. NMe_4SCN and NMe_4SeCN were synthesized from NMe_4Cl, and NaSCN and KSeCN, respectively, and purified by multiple recrystallization.

Crystals of $(TTF)(SCN)_x$ and $(TTF)(SeCN)_y$ were grown by metathesis reactions in acetonitrile using diffusion vessels. The subscripts x and y are the

mole ratios of SCN and SeCN to TTF, respectively. The $(TTF)(SCN)_x$ crystals were long, thin, and extremely fragile. The $(TTF)(SeCN)_y$ crystals were longer and thicker. The crystals exhibited the same morphology with eight faces developed at every 45° around an octagonal prism. Single-crystal x-ray diffraction measurements on both salts were performed.[8]

For $(TTF)(SeCN)_y$, rotation, Weissenberg, and precession measurements yield a tetragonal (or pseudotetragonal) unit cell with a nonstandard C-centered lattice constant of $a_0 = b_0 = (\sqrt{2})(11.28\ \text{Å}) = 15.95\ \text{Å}$. The C-centered lattice is used to facilitate comparison with the $(TTF)_7(I)_5$ structure.[9] The c_0 tetragonal axis shows two spacings of 3.60 ± 0.01 Å (TTF spacing) and 6.17 ± 0.02 Å (SeCN spacing). Within experimental accuracy these spacings yield a value of $y = 0.584 \approx \frac{7}{12}$, i.e., $(TTF)_{12}(SeCN)_7$, and are consistent with a unit cell spacing $c_0 = 43.2$ Å. The value of $y = 0.58$ differs beyond experimental error from that found by Wudl[6] ($y = 0.55 \simeq \frac{6}{11}$). The appearance of diffuse streaks from the second- and third-order SeCN lines in needle rotation photographs may be due to large amplitude thermal vibrations or disorder in the SeCN chains.

In the case of the $(TTF)(SCN)_x$, the x-ray studies yield a tetragonal (or pseudotetragonal) unit cell with a C-centered lattice constant of $a_0 = b_0$ $(\sqrt{2})$ (11.11 Å) = 15.71 Å. The c_0 tetragonal axis also shows two spacings of 3.61 ± 0.03 Å (TTF spacing) and 6.15 ± 0.03 Å (SCN spacings). These yield $x = 0.587$, again consistent with a $(TTF)_{12}(SCN)_7$ stoichiometry and a unit cell spacing $c_0 = 43.3$ Å. The TTF stacks are eclipsed and show no disorder in both salts. A summary of the structural data is given in Table I.

Thermoelectric power (TEP) and four-probe electrical conductivity measurements were performed as described elsewhere.[3] Electrical contact to the single-crystal samples was made using evaporated gold or aquadag. Typical contact resistances were of the order of 15 to 100 ohms. Silver paint was found to form insulating contacts. ESR measurements were carried out with a Varian X-band spectrometer equipped with an Air Products temperature probe modified by a vacuum shield to prevent changes in Q value of the cavity. The optical reflectivity was measured using a microspectrophotometer coupled to a Beckman DK-2A monochrometer. Reflectivity data could not be obtained on $(TTF)_{12}(SCN)_7$ because of the unavailability of sufficiently large crystals.

RESULTS

The magnitudes of the room-temperature longitudinal conductivities are high with $\sigma_{RT} = 550 \pm 250$ $\Omega^{-1}\,\text{cm}^{-1}$ for $(TTF)_{12}(SCN)_7$ and $\sigma_{RT} = 750 \pm 150$ $\Omega^{-1}\,\text{cm}^{-1}$ for $(TTF)_{12}(SeCN)_7$. These values are comparable with those found for $(TTF)(TCNQ)$,[2] $\sigma_{RT} \sim 500\ \Omega^{-1}\,\text{cm}^{-1}$, and are higher than any room-temperature value found in the single-carrier TCNQ salts, e.g., $\sigma_{RT} \sim 380\ \Omega^{-1}\,\text{cm}^{-1}$ for N-methylphenazinium tetracyanoquinodimethane $(NMP)(TCNQ)$.[10] The higher value found in the SeCN salt as compared to the SCN salt may reflect a larger contribution to screening from the higher polarizability of selenium as compared to sulfur. The high conductivities are surprising in view of the large TTF spacing (3.60 Å). However, the eclipsed nature of the stacks maximizes orbital overlap, and hence, counteracts the effect of the larger separation. Using the carrier concentration $N = 2.55 \times 10^{21}\,\text{cm}^{-3}$ from x-ray data, a tight-binding calculation of the mean free path $\lambda_F = \pi\hbar\sigma/2Ne^2a$ leads to values of the order of 7 Å.

Figure 1 shows the temperature dependence of the four-probe single-crystal resistivity along the needle axis for $(TTF)_{12}(SCN)_7$ and $(TTF)_{12}(SeCN)_7$ at high temperatures ($T > 150\,°\text{K}$). The resistivities decrease with decreasing temperature over the temperature range 250–350 °K.

While the $(TTF)_{12}(SCN)_7$ resistivity is seen to decrease approximately linearly with decreasing temperature in the range 260–350 °K (to within experimental accuracy of ± 0.5%), the $(TTF)_{12}(SeCN)_7$ resistivity decreases with temperature in a superlinear fashion in the same temperature range. The data for $(TTF)_{12}(SeCN)_7$ can be described by an equation of the form

$$\rho(T) = A + BT^n. \tag{1}$$

Values of n within the range 4–6 gave least-squares fits whose standard deviations were within experimental error. It is interesting to note

TABLE I. Summary of structural data for $(TTF)_{12}(SCN)_7$ and $(TTF)_{12}(SeCN)_7$.

	$a_0 = b_0$ (Å)	c_0 (Å)	TTF spacing (Å)	Anion spacing (Å)
$(TTF)_{12}(SCN)_7$	15.71	43.3	3.61 ± 0.01	6.15 ± 0.03
$(TTF)_{12}(SeCN)_7$	15.95	43.2	3.60 ± 0.01	6.17 ± 0.02

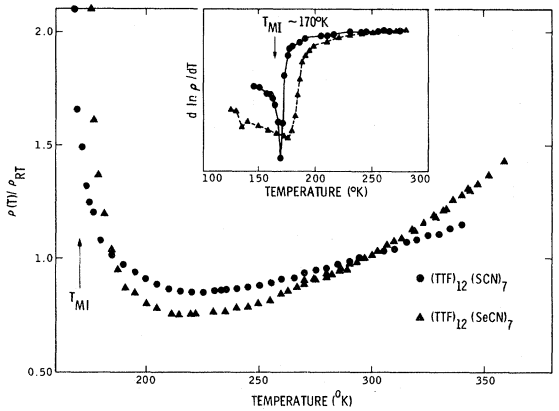

FIG. 1. Temperature dependence of the normalized resistivity of $(TTF)_{12}(SCN)_7$-●-●-●- and $(TTF)_{12}(SeCN)_7$-▲-▲-▲-. The inset shows the logarithmic derivative of the resistivity versus temperature.

that the best fit to the data corresponds to $n=5$ which can be compared, for example, to the value $n=4$ for the single-carrier anion-radical stack system NMP-TCNQ,[10] and to the value $n=2.33$ for the two-carrier anion-radical–cation-radical stack system (TTF)(TCNQ).[11] While no significance can be attached at present to any particular value of n within the range specified, it is clear that $n>1$ for $(TTF)_{12}(SeCN)_7$.

The peak values for the conductivity occur at a temperature, $T_{pk} \simeq 230 \pm 10$ °K, with values of $\sigma(T_{pk})/\sigma_{RT} \sim 1.1$–$1.3$. This ratio is quite similar to that found in other single-carrier organic charge transfer salts, e.g., (NMP)(TCNQ), but quite different from that found in two-carrier materials such as (TTF)(TCNQ).[12] A metal-insulator (MI) transition occurs for both compounds at a temperature $T_{MI} \approx 170$ °K. The value of T_{MI} was determined from plots of $d(\ln\rho)/dT$ versus temperature (see inset, Fig. 1). The temperature at which a minimum in the logarithmic derivative occurs is closely related to the true thermodynamic transition temperature.[12] These plots also reveal that the transition is quite sharp in $(TTF)_{12}(SCN)_7$ ($\Delta T \simeq 1$ °K) compared to $(TTF)_{12}(SeCN)_7$, $\Delta T \simeq 5$ °K. This may reflect larger disorder of the SeCN salt. It should be noted that $T_{pk} > T_{MI}$ in our materials as well as in other organic charge-transfer salts. The variation in T_{MI} and T_{pk} among different samples (see Table II) obscures the temperature difference, $T_{MI}(Se) - T_{MI}(S) \equiv \Delta T_{MI}$. Nevertheless, the trend in the data suggest that $\Delta T_{MI} \sim 5$ °K. At low temperatures ($T < 150$ °K), the materials exhibit semiconducting behavior. Figure 2 shows the temperature dependence of the resistivity in the low-temperature region. The inset to Fig. 2 shows the temperature dependence of the activation energy $\Delta(T)$ for a crystal of $(TTF)_{12}(SeCN)_7$, as computed from

$$\Delta(T) = T[\ln\rho(T) - \ln\rho_0], \tag{2}$$

using the Arrhenius equation, $\rho_0(T) = \rho_0 e^{\Delta(T)/T}$. The resulting temperature dependence of $\Delta(T)$ depends on the particular normalization procedure used[12] as shown in the inset. However, the zero-temperature activation energy $\Delta(0)$ is independent of the normalization, and the values obtained are $\Delta(0) = 1025 \pm 75$ °K for $(TTF)_{12}(SCN)_7$ and $\Delta(0) = 950 \pm 50$ °K for $(TTF)_{12}(SeCN)_7$. The ratio of the zero-temperature gap to the transition temperature, $2\Delta(0)/T_{MI}$, varies from 10–13 and is similar to that observed in other organic charge-transfer salts,[12] but considerably greater than the value of 3.5 predicted by the mean-field theory of the Peierls instability.[13] The deviations from the mean-field value in the charge transfer salts are thought to be due to their one-dimensional character.[14]

The samples were thermally cycled several times and no evidence of hysteresis was observed.

Our resistivity data are to be contrasted with those of Wudl *et al.*,[6] who did not observe metal-like temperature dependence of the resistivity for their SeCN salt near room temperature. Also, our room-temperature conductivities were consistently higher than those observed by Wudl *et al.*[6] by a factor on the order of 50 for the SeCN salt, and approximately two for the SCN salt. A summary of the conductivity results is given in Table II.

Figure 3 shows the temperature dependence of the absolute thermoelectric power (TEP) α along the needle axis. The room-temperature TEP of both salts is small and positive, ~9 μV/°K indicative of hole conduction along the TTF chains (as

TABLE II. Summary of electrical conductivity data.

	T_{MI} (°K)	T_{pk} (°K)	σ_{RT} (Ω^{-1}cm^{-1})	$\Delta(0)$ (°K)	$2\Delta(0)/T_{MI}$
$(TTF)_{12}(SCN)_7$	169 ± 1	225 ± 5	550 ± 250	1025 ± 75	12 ± 1
$(TTF)_{12}(SeCN)_7$	173 ± 5	230 ± 10	750 ± 150	950 ± 50	11 ± 1

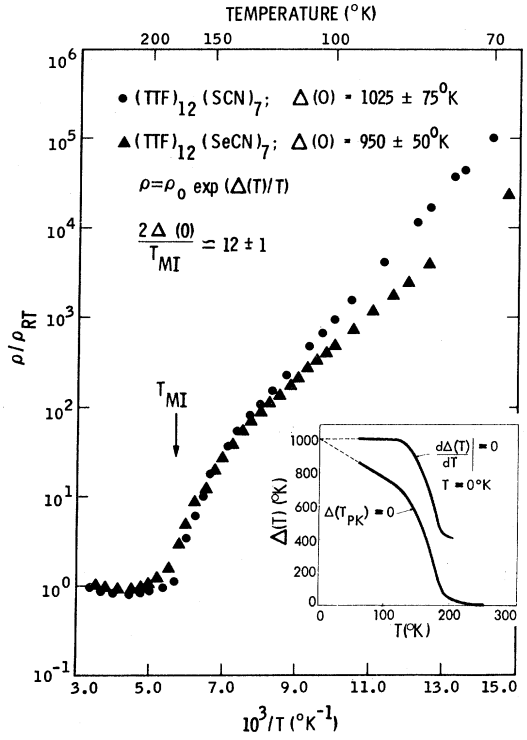

FIG. 2. Temperature dependence of the normalized resistivity of $(TTF)_{12}(SCN)_7$-●-●-●- and $(TTF)_{12}(SeCN)_7$-▲-▲-▲-. The inset shows the temperature dependence of the activation energy for two different normalizations for the SeCN salt. T_{pk} is the temperature at which the conductivity is a maximum.

expected for a more than half-filled electron band). A similar value,[3] $\sim +6.5$ μV/°K was found in $(TTF)_7(I)_5$. In the region above 190 °K, the TEP of both salts decreases linearly with decreasing temperature. A least-squares fit of the $(TTF)_{12}(SCN)_7$ data above 190 °K, gives the temperature dependence of the TEP (in μV/°K) as

$$\alpha(T) = 0.029T - 0.2. \qquad (3)$$

It is seen that the TEP extrapolates to zero within 0.2 μV/°K at $T = 0$ °K, as is the case for simple metals. A zero intercept is also observed in (TTF)(TCNQ).[15] A similar fit to the $(TTF)_{12}(SeCN)_7$ data above 190 °K yields

$$\alpha(T) = 0.012T + 6.3. \qquad (4)$$

The +6.3 μV/°K value at $T = 0$ °K suggests a positive contribution to the TEP from carriers moving in a band with energy-dependent relaxation times.

In one dimension, and neglecting energy-dependent scattering processes, the TEP in the tight-binding approximation is given by

$$\alpha = [(\pi k_B)^2 T/6et]\cos\tfrac{1}{2}\pi\rho/(1-\cos^2\tfrac{1}{2}\pi\rho), \qquad (5)$$

where t is the intermolecular transfer integral and

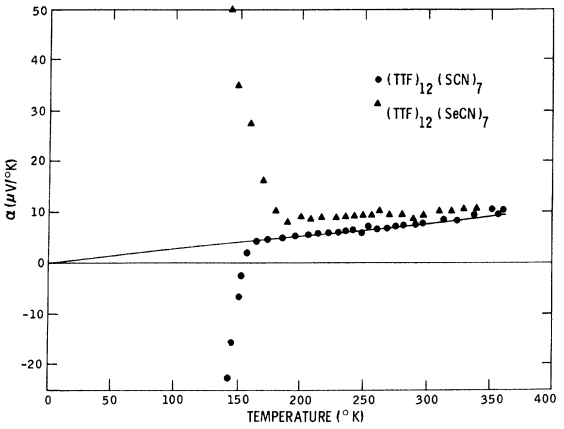

FIG. 3. Temperature dependence of the TEP of $(TTF)_{12}(SCN)_7$-●-●-●- and $(TTF)_{12}(SeCN)_7$-▲-▲-▲-. The solid line is the least-squares fit, Eq. (3).

ρ is the hole filling factor. With a hole filling factor of $\frac{7}{12}$, a fit of the SCN experimental data [Eq. (3)] to Eq. (5) gives a bandwidth, $E_0 = 4t$, of 1.94 eV. The use of the room temperature TEP of the SeCN salt (ignoring the nonzero intercept) and Eq. (5) yields $E_0 = 1.56$ eV. The Fermi energy for holes may be calculated within the tight-binding approximation using the dispersion relation, the filling factor, and the bandwidth. In the case of $(TTF)_{12}(SCN)_7$, this yields $\epsilon_F^h = 0.34$ eV (ϵ_F^h measured positive and downwards from the top of the occupied band). For comparison, the equation for the TEP for free holes in one dimension, $\mathrm{TEP} = \pi^2 k_B^2 T/6e\epsilon_F^h$, yields $\epsilon_F^h = 0.42$ eV when applied to $(TTF)_{12}(SCN)_7$.

Significant deviations from linearity in α vs tem-

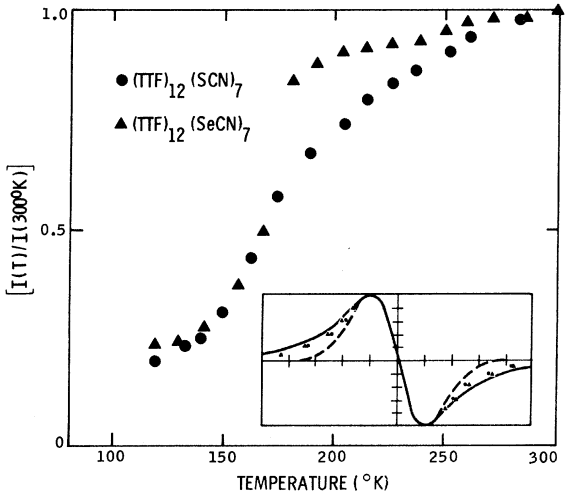

FIG. 4. Temperature dependence of the normalized ESR intensity of $(TTF)_{12}(SCN)_7$-●-●-●- and $(TTF)_{12}(SeCN)_7$-▲-▲-▲-. Inset compares the data to a Lorentzian (——) and Gaussian (----) line shape.

perature occur about 10 °K above T_{MI} for both compounds. Below T_{MI} the TEP becomes large and negative for $(TTF)_{12}(SCN)_7$, and large and positive for $(TTF)_{12}(SeCN)_7$ indicating a low-temperature nonconducting state in each case.

One might attempt to understand the low-temperature TEP in terms of a Peierls-distorted state. Since the Peierls gap opens up at the Fermi energy, the energy states above the gap form a band narrower than that formed by those below the gap for the present case of a more-than-half-filled undistorted band. The mobility of the carriers (electrons) in the upper (conduction) band is therefore smaller than that of the carriers (holes) in the lower valence band, and one would expect a large and positive thermopower for such an intrinsic semiconductor, as observed in the case of the SeCN salt. The negative thermopower for the SCN salt, however, cannot be explained within this framework, and it appears likely that impurities dominate the low-temperature thermopowers.

Figure 4 shows the temperature dependence of the ESR intensity normalized to the room-temperature value for a random orientation of crystals for each salt. The room-temperature g values are 2.0075 and 2.0080 for $(TTF)_{12}(SCN)_7$ and $(TTF)_{12}(SeCN)_7$, respectively. The line shape for both salts is primarily Lorentzian (see inset, Fig. 4). The room-temperature linewidths are 15 and 17G for $(TTF)_{12}(SCN)_7$ and $(TTF)_{12}(SeCN)_7$, respectively. These linewidths are substantially smaller than that observed in $(TTF)_7(I)_5$ where spin-orbit effects are stronger.[3]

The ESR intensity $I(T)$ decreases with decreasing temperature for both salts with a sharp drop occurring at 175 °K in each case. An excellent least-squares fit of the data above 175 °K can be made to an equation of the form

$$I(T) = (C/T)e^{-\delta/T}, \tag{6}$$

with $\delta = 550 \pm 100$ °K for $(TTF)_{12}(SCN)_7$ and $\delta = 350 \pm 50$ °K for $(TTF)_{12}(SeCN)_7$. These values are similar to the value of δ (= 360 °K) observed in $(TTF)_7(I)_5$.[3]

Equation (6) implies the existence of an energy gap which is puzzling in view of the metal-like features of the conductivity, thermoelectric power, and reflectivity (see below) in this temperature range. Another mechanism which can give a decrease in susceptibility with decreasing temperature involves the effects of fluctuations on the Peierls transition in a one-dimensional system, as suggested by Lee, Rice, and Anderson.[14] In the latter case, an energy gap is not present and the decreasing susceptibility reflects a decrease in the density of states at the Fermi energy. While this model is consistent with the metal-like features mentioned above, the ESR intensity above the metal-insulator transition T_{MI} does not decrease as rapidly with temperature as is required by the Lee-Rice-Anderson theory. The exact nature of the magnetic excitations cannot, therefore, be specified at present.

At ~120 °K, a second component in the ESR signal is observed which persists to the lowest temperatures measured (~5 °K). This second component, observed in our randomly oriented crystals, probably reflects an anisotropic g value.[6]

Figure 5 shows the temperature dependence of the ESR linewidth. The linewidth of $(TTF)_{12}(SCN)_7$ is constant above 200 °K while the linewidth of $(TTF)_{12}(SeCN)_7$ decreases linearly with decreasing temperature down to 200 °K. This latter temperature dependence, as well as the Lorentzian line shape, is suggestive of spin-lattice relaxation processes in a metal when spin-orbit coupling is significant. One expects more back charge transfer in $(TTF)_{12}(SeCN)_7$ than in $(TTF)_{12}(SCN)_7$ since the ionization potential of $SeCN^-$ should be less than that of SCN^-. Also, uv-visible solution spectra[16] indicate that no appreciable back charge transfer takes place in $(TTF)_{12}(SCN)_7$ while a small finite amount is present in $(TTF)_{12}(SeCN)_7$. This effect, coupled to the large-spin orbit coupling constant of Se suggests the spin-lattice relaxation mechanism for the SeCN salt.

Below 200 °K, the linewidths of both salts decrease sharply. No hysteresis effects are observed in either the ESR intensity or linewidth upon thermal cycling

Figure 6 shows the reflectivity of $(TTF)_{12}(SeCN)_7$ single crystals for light polarized both parallel ($R_{\parallel}$) and perpendicular ($R_{\perp}$) to the needle axis. The

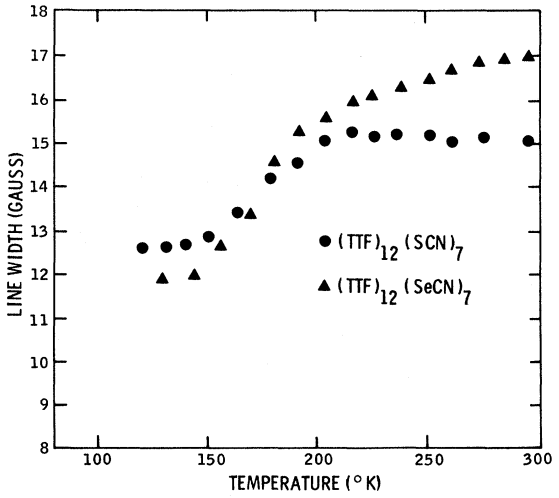

FIG. 5. Temperature dependence of the ESR linewidth for $(TTF)_{12}(SCN)_7$-●-●-●- and $(TTF)_{12}(SeCN)_7$-▲-▲-▲-.

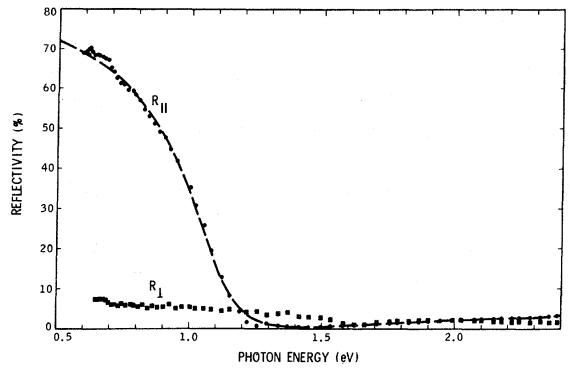

FIG. 6. Reflectivity of $(TTF)_{12}(SeCN)_7$, measured at room temperature for light polarized parallel, $R_{\parallel}$-●-●-, and perpendicular, $R_{\perp}$-■-■-, to the conducting axis. The dashed line represents a least-squares fit to the Drude Model, Eq. (8).

reflectivity parallel to the needle axis shows a pronounced increase to quite high values (~70%) as the photon energy is decreased. In view of the metal-like features of the conductivity and TEP, this shoulder could be due to a plasma edge associated with Drude behavior. Therefore, the $R_{\parallel}$ data were fit to a Drude model using

$$R_{\parallel}=\frac{1+|\epsilon|-[2(|\epsilon|+\epsilon_1)]^{1/2}}{1+|\epsilon|+[2(|\epsilon|+\epsilon_1)]^{1/2}}, \tag{7}$$

where $|\epsilon|=(\epsilon_1^2+\epsilon_2^2)^{1/2}$ and the Drude dielectric function is given by

$$\epsilon^D(\omega)=\epsilon_c-\omega_p^2/(\omega^2+i\omega/\tau_{op})=\epsilon_1+i\epsilon_2. \tag{8}$$

ϵ_c contains contributions to the polarizability from core electrons, $\omega_p=(4\pi N_h e^2/m^*)^{1/2}$ is the plasma frequency, N_h is the density of holes, m^* is the optical effective mass, and τ_{op} is the optical relaxation time. The fit yields the following parameters: $\epsilon_c=2.63$, $\hbar\omega_p=1.78$ eV, and $\tau_{op}=2.86\times10^{-15}$ sec. Comparing $\hbar\omega_p$ with the free electron value using $N_h=2.55\times10^{21}$ cm^{-3} yields an effective-mass ratio $m^*/m_0=1.1$. The optical conductivity

$$\sigma_{op}=\omega_p^2\tau_{op}/4\pi \tag{9}$$

is $\sigma_{op}=1.9\times10^3\ \Omega^{-1}$ cm^{-1}, which is three times the dc value.

The bandwidth may be calculated from the effective mass and compared to that obtained from the thermoelectric power measurements. For a partially filled tight-binding band, the bandwidth is given by

$$E_0=\pi\hbar^2/m^*a^2R, \tag{10}$$

where $R=\sin\frac{1}{2}\pi\rho$, and the hole filling factor ρ is $\frac{7}{12}$ for $(TTF)_{12}(SeCN)_7$. Equation (10) yields $E_0\sim2.1$ eV, which is several times greater than that observed in $(TTF)(TCNQ)$[2] and is in good agreement with the value obtained from the TEP data using the tight-binding model [Eq. (5)].

An important point must be made concerning the above analysis and corresponding numbers. The fit to Eq. (8) is by no means unique. A fit, almost as good (in a statistical sense), can be made to a Lorentz model using a single oscillator

$$\epsilon^L(\omega)=\epsilon_c^L+\omega_{pi}^2/[(\omega_i^2-\omega^2)-i\omega/\tau_i], \tag{11}$$

with $\epsilon_c^L=2.64$, $\hbar\omega_{pi}=1.79$ eV, $\tau_i=2.86\times10^{-15}$ sec, and $\hbar\omega_i=0.08$ eV. Therefore, care must be exercised in the interpretation of the reflectivity data. The high value of the reflectivity at the lowest energy measured, as well as the temperature dependence of the conductivity and TEP, argues against a strong low-energy transition, but far-ir reflectance measurements will be necessary to resolve unambiguously this question. It should be noted that $\hbar\omega_p\lesssim E_0$ and, thus, the question of the equality of the optical relaxation time τ_{op} with that characteristic of electron-phonon scattering processes τ_{ep} emerges. Hopfield[17] has shown that the dimensionless electron-phonon coupling constants λ_i may be determined from optical and dc parameters for $T\gg\Theta_D$

$$\begin{aligned}\lambda_1&=(\hbar/2\pi k_B T)(\tau_{ep})^{-1},\\ \lambda_2&=(\hbar/2\pi k_B)(\omega_p^2/4\pi)\partial\rho_{dc}/\partial T,\end{aligned} \tag{12}$$

where $\tau_{op}^{-1}=\tau_{ep}^{-1}+\tau_{other}^{-1}$. If only electron-phonon contributions to τ are important, then λ_1 should equal λ_2. Using $\tau_{op}=\tau_{ep}$ and ω_p as determined from Eq. (8) with $(\partial\rho_{dc}/\partial T)_{T=300\,^\circ K}=3.21\times10^{-6}\ \Omega$ cm/°K, yiekds $\lambda_1=1.4$ and $\lambda_2=2.6$. Although the difference in magnitude between λ_1 and λ_2 is smaller than that found for $(TTF)(TCNQ)$,[18] we believe this difference is significant and that contributions from processes involving other than electron-phonon scattering may be important. Furthermore, the magnitudes of the λ_i are anomalously large. The source of the large value of λ_1 is likely the use of $\tau_{op}=\tau_{ep}$. If one were to include an additional relaxation time corresponding to τ_{other}, say, from electron-electron scattering, λ_1 would be reduced to a more reasonable value. The source of the large value of λ_2 is the $T^n(n>1)$ dependence of the resistivity [Eq. (1)], which itself is suggestive of an additional scattering mechanism.

CONCLUSIONS

The electrical, magnetic, and optical properties of $(TTF)_{12}(SCN)_7$ and $(TTF)_{12}(SeCN)_7$ have been measured. These materials are highly conducting with many metal-like features.

The magnitude of the room-temperature conductivity of $(TTF)_{12}(XCN)_7$(X = S or Se) is higher than that observed in any TCNQ salt not containing TTF

or any of its derivatives. Analysis of the data indicates that charge transport is by holes in a partially filled band of bandwidth, $E_0 \sim 1-2$ eV. We believe this large bandwidth results from the improved orbital overlap of the large $3p\pi$ sulfur orbitals of TTF in an eclipsed stack structure. This supports the theoretical results of Salahub *et al.*[19] who carried out self-consistent-field–$X\alpha$–scattered-wave (SCF–$X\alpha$–SW) molecular-orbital calculations of dimers of TTF in eclipsed as well as slipped geometries. A bandwidth of 0.99 eV resulted from eclipsed stacking while a much smaller bandwidth of 0.20 eV was found for slipped stacking [as occurs in (TTF)(TCNQ)].

The conductivity of $(TTF)_{12}(XCN)_7$ peaks at $T_{pk} \sim 200$ °K and undergoes a metal-insulator transition at $T_{MI} \sim 170$ °K. This value of T_{MI} is quite similar to those observed in other single-carrier quasi-one-dimensional conductors, yet is appreciably higher than the corresponding temperatures in the two-carrier systems.[12] This suggests that there may be a synergistic effect present in the two-carrier conducting salts which stabilizes the metallic state. An example of a possible stabilizing factor would be enhanced interchain coupling resulting from better screening along one chain by the delocalized carriers on the adjacent chain. The small intermolecular spacings characteristic of two-carrier systems contribute significantly to the stability of the metallic state, while eclipsed stacking does not seem to play an important role. The exact nature of the transition in $(TTF)_{12}(XCN)_7$ is unknown although the insulating and weakly magnetic nature of the low-temperature state suggests a Peierls type of transition.

ACKNOWLEDGMENTS

We are indebted to C. J. Fritchie, Jr. for communicating his x-ray results on the (TTF)(pseudohalides) and are grateful to E. Washington for assistance in the synthesis program. We wish to thank A. Rembaum for helpful discussions, and F. Wudl, G. A. Thomas, and W. M. Walsh, Jr. for discussing their results prior to publication.

---

† This paper represents one phase of research performed by the Jet Propulsion Laboratory, California Institute of Technology sponsored by NASA Contract NAS7-100.

[1] I. F. Schegolev, Phys. Status Solidi A 12, 9 (1972); H. R. Zeller, Adv. Solid State Phys. 13, 31 (1973).

[2] For a general review, see *Low Dimensional Cooperative Phenomena, The Possibility of High-Temperature Superconductivity*, edited by H. J. Keller (Plenum, New York, 1975), and references therein.

[3] R. B. Somoano, A. Gupta, V. Hadek, T. Datta, M. Jones, R. Deck, and A. M. Hermann, J. Chem. Phys. 63, 4970 (1975).

[4] R. J. Warmack, T. A. Callcott, and C. R. Watson, Phys. Rev. B 12, 3336 (1975).

[5] S. J. La Placa, P. W. R. Corfield, R. Thomas, and B. A. Scott, Solid State Commun. 17, 635 (1975).

[6] F. Wudl, J. Am. Chem. Soc. 97, 1962 (1975); F. Wudl, G. A. Thomas, D. E. Schafer, and W. M. Walsh, Jr., J. Liq. Mol. Cryst. (1976); private communication.

[7] L. R. Melby, J. Org. Chem. 39, 2456 (1974).

[8] C. J. Fritchie, Jr. (private communication).

[9] J. J. Daly and F. Sanz, Acta Crystallogr. B 31, 620 (1975); C. K. Johnson and Charles R. Watson, Jr., J. Chem. Phys. 64, 2271 (1976).

[10] L. B. Coleman, J. A. Cohen, A. F. Garito, and A. J. Heeger, Phys. Rev. B 7, 2122 (1973).

[11] R. P. Groff, A. Suna, and R. E. Merrifield, Phys. Rev. Lett. 33, 418 (1974).

[12] S. Etemad, Phys. Rev. B 13, 2254 (1976); S. Etemad, T. Penney, E. M. Engler, B. A. Scott, and P. E. Seider, Phys. Rev. Lett. 34, 741 (1975).

[13] M. J. Rice and S. Strässler, Solid State Commun. 13, 125 (1973).

[14] P. Lee, T. M. Rice, and P. W. Anderson, Phys. Rev. Lett. 31, 462 (1973).

[15] P. M. Chaikin, J. F. Kwak, T. E. Jones, A. F. Garito, and A. J. Heeger, Phys. Rev. Lett. 31, 601 (1973).

[16] A. Gupta and R. B. Somoano (unpublished).

[17] J. J. Hopfield, Comments Solid State Phys. 3, 48 (1970).

[18] P. M. Grant, R. L. Greene, G. C. Wrighton, and G. Castro, Phys. Rev. Lett. 31, 1311 (1973).

[19] D. R. Salahub, R. P. Messmer, and F. Herman, Phys. Rev. B 13, 4252 (1976).